Research Article

DESIGN AND ANALYSIS OF RECONFIGURABLE ULTRA-WIDE BAND PASS FILTER INTEGRATION WITH NOTCH BAND

Salah M. OBAID[1,*], *Mithaq N. RAHEEMA*[2], *Raaed T. HAMMED*[1]

[1]Department of Electrical Engineering, University of Technology, Baghdad, Iraq
[2]Department of Prosthetics & Orthotics Engineering, College of Engineering, University of Kerbala, Kerbala, Iraq

eee.20.13@grad.uotechnology.edu.iq, methaq.n.rhiama@uokerbala.edu.iq, raaed.t.hammed@uotechnology.edu.iq

[*]Corresponding author: Salah Mahdi; eee.20.13@grad.uotechnology.edu.iq

DOI: 10.15598/aeee.v23i3.250303

Article history: Received Mar 1, 2025; Revised May 23, 2025; Accepted Jul 7, 2025; Published Sep 30, 2025.

Abstract. *Advancements in ultra-wideband reconfigurable band-pass filters (BPF) with notch band function are required for modern communication systems operating across a broad frequency spectrum. This paper introduces an innovative design of a reconfigurable UWB BPF with notch functionality covering two separate operating states: 1st operating frequency band of 3.7 GHz – 13 GHz with good insertion and return losses, at approximately 0.9 dB/58 dB respectively, and the 2nd operating frequency band from 2.7 GHz to 15 GHz incorporating 5.1 GHz – 5.3 GHz notch band with insertion and return losses of 1.3 dB/57 dB respectively, using PIN/Varactor switches. Subsequently, a notch filter is strategically integrated into the design to suppress unwanted frequencies, enhancing the filter's selectivity and interference rejection capabilities. An experimental prototype for the reconfigurable filter with PIN diodes was fabricated to validate the effectiveness of the proposed design, demonstrating its suitability for UWB communication applications. Notably, the filter exhibits UWB characteristics, with a broad passband covering a wide frequency range with notch filtering to attenuate interfering signals. The compact size of the filter design 23.4 mm × 8.7 mm ensures practical integration into communication systems.*

Keywords

Band Pass, Ultra-Wide Band, Notch Band, Reconfigurable, PIN diode, Varactor switch.

1. Introduction

The requirements of wireless communication and signal processing systems have forced the development of reconfigurable filter designs. These filters present many advantages, including size and cost reduction, adaptability, and flexibility, making these filters important components in modern communication systems for instance, Ultra-wideband (UWB), satellite, 4G/5G, WiMAX, WLAN, and radar. UWB technology supports high-data-rate wireless communication within a broad frequency range. This technique works with low power consumption, accurate positioning, and minimum interference due to these advantages. UWB is ideal for short-range applications such as radar, sensing, and data transfer.

Several studies have focused on the UWB technique, R.T. Hammed presented a compact E-shaped UWB band-pass filter. To improve lower stopband selectivity, a sixth-order filter was designed and measured, achieving 50 dB attenuation beyond the passband over the UWB frequency range [1]. In another approach, a compact multi-band UWB band-pass filter containing five quarter-wavelength short-circuited stubs and three U-shaped open-circuited stubs was proposed. The notch bands effectively eliminate the interference at 4.6 GHz, 5.6 GHz, and 8.5 GHz [2]. In another study, a parallel-coupled-line UWB band-pass filter was designed and measured, created from three parallel-coupled lines at a frequency of 6.9 GHz [3]. Another article proposed a compact planar notch UWB band-pass filter

with metamaterial and Substrate-Integrated Waveguide (SIW) technique. The filter eliminates WLAN frequencies from 5 GHz to 5.7 GHz [4]. Reconfigurable filters are an essential element in dynamic frequency conditions. Conventional reconfigurability functions contain frequency and bandwidth, while common reconfiguring components include PIN diodes, varactor diodes, and MEMS switches. Varactor diodes and PIN diodes are preferences due to their simplicity of integration, appropriateness for high frequencies, and low power utilization. Varactor diodes act as voltage-controlled capacitors; their capacitance value varies according to the applied reverse bias voltage. Varactor diodes are used to tune the filter's response by regulating the reverse voltage through the varactor diode with a specific range of capacitance values [5]. While PIN diodes are conducted as current-controlled switches, their resistance value change according to the forward bias current. PIN diodes work as high-frequency switches in reconfigurable filters, exchanging ON and OFF states with forward and reverse bias voltages [6].

To investigate the reconfigurability functions that microstrip filters can be operated. Many studies have been considered. For Reconfigurable wide band with notch bands filter studies, among these techniques, a reconfigurable UWB monopole antenna with triple narrow band-notched characteristics for cognitive radio applications has been presented in [7]. The notched frequencies are achieved using a Defected Microstrip Structure (DMS). The filter operates over a frequency band of 3.1 GHz to 14 GHz with three notched bands 4.2 GHz to 6.2 GHz, 6.6 GHz to 7.0 GHz, and 12.2 GHz to 14 GHz [7]. A method involves using a microstrip filter that can switch between band-pass and band-stop responses using square ring resonators and open-circuited stub resonators. The design operated at a frequency 11.2 to 14.5 GHz. Diodes SMP12341 RF-PIN were used to perform the reconfigurability function [8]. Authors in another study presented a model and analysis of a compact reconfigurable low-pass/band-pass filter based on a negative refractive index metamaterial transmission line. Reconfigurability is achieved by incorporating switches in the cells. The low pass filter has a 3-dB cut-off frequency of 3.25 GHz. On the other hand, the band-pass filter is centered at 3.65 GHz [9]. On the other hand, another research introduced a very compact planar reconfigurable band-pass to band-pass/low-pass filter designed for 5G applications, covering the 0 to 1 GHz and 3.4 to 3.8 GHz spectrum [10]. In another article, the authors present a reconfigurable loop-based filter capable of compound reconfiguration. The filter is designed to function as either a band-stop or band-pass filter by cascading the resonator to the transmission line connecting the source and load. Two BAR64-03W PIN diodes are used to enable reconfiguration [11]. Another study introduces two on-chip band stop/band pass reconfigurable filters operating in C and X bands. The filters are proposed on a silicon substrate, and reconfigurability is accomplished using semiconductor-distributed doped areas. As a proof of model, 5 GHz and 10 GHz filters were constructed [12]. Another proposed design introduces a dual wideband filter that can switch between band-pass and band-stop modes using PIN switches. The band stop filter operates in the frequency range of 1.3 - 3.2 GHz and 5.6 - 7.5 GHz [13]. In another approach, a reconfigurable filtering antenna is introduced for wireless communication techniques. The incorporation of MA4AGBLP912 PIN switches enables the filter to switch between an UWB and a dual-band state. In the dual-band state, the filter works at 3.35 GHz and 5.2 GHz [14]. Moreover, another article provides a comprehensive review of design methods for reconfigurable band-pass filters operating at 3.4 – 3.77 GHz [15]. However, different work explores a filter designed for wide-band and tri-band pass filter applications. The wide band structure is providing a passband from 2 GHz to 6.1 GHz. The proposed tri-band band-pass filter presents pass bands at 2.4 GHz, 3.5 GHz, and 5.2 GHz. SMP1340-079LF PIN effectively switches the operation between wide-band and tri-band modes [16].

A dual-band radio frequency (RF) reconfigurable filter based on quarter-wavelength coupled lines and open stubs has been presented. Primarily, an even–odd mode analysis was achieved for the proposed design. RF filter with varactor diodes performs tuning function from 2.06–2.40 GHz and 5.44–5.84 GHz with system size of 45.5 mm × 29.4 mm [17]. Authors in another study present a new design, compact UWB filtering antenna with dimensions (32 x 27) mm, incorporates a stepped-flower patch with a stub-based filter using six PIN diodes to create a reconfigurable notch band. Operating from 3.52 to 10.1 GHz [18]. A new design of a reconfigurable bandpass filter constructed with varactor diodes has been proposed in [19]. The S_{21} frequency range shifts from 2.25 GHz to 2.6 GHz as the input reverse voltage (V_{in}) differs from 0 to 5 V. The filter dimensions are 61.1 mm x 48.2 mm is suitable for space-constrained RF systems.

The featured summary of the different reconfiguring switches used in previous research is shown in Table 1.

The tuning components within the structure of reconfigurable filters act as fundamental elements. These switches are carefully engineered to apply adjustments in particular characteristics of the reconfigurable filter. This means confirming compatibility with various communication techniques, frequency bands, and varying environmental conditions.

This research includes a filter design for a reconfigurable UWB filter, precisely directing to assess the effect of PIN switches in contrast to conventional inductors and capacitors. Moreover, it integrates a reconfig-

Tab. 1: Detailed Features of the Different Reconfiguring Switches used in Previous Researches.

Ref.	Switch model	Frequency band	Features
[7]	Varactor (SMV2023)	up to 10 GHz	$Rs = 1.6\ \Omega$, $Ct = 1.29$ to 12.23 pF, $V\ bias = 20$ to $0\ v$
[8]	PIN (HMPP3890)	up to 6 GHz	$Rs = 2.5\ \Omega$, $Cj = 0.3$ pF
[7, 9]	PIN (BAR64)	1 MHz to 3 GHz	$Rs = 2.1\ \Omega$, $Cj = 0.17$ pF, $Rj = 3\ k\Omega$
[10, 18]	PIN (MA4LP912)	up to 40 GHz	$Rs = 4\ \Omega$, $Cj = 0.028$ pF, $Rj = 10\ k\Omega$
[11]	PIN (SMP1340)	10 MHz to 10 GHz	$Rs = 1\ \Omega$, $Cj = 0.3$ pF, $Rj = 65\ k\Omega$
[12, 13, 15, 17]	Varactor (SMV1405)	up to 10 GHz	$Rs = 0.8\ \Omega$, $Ct = 0.62$ to 2.67 pF, $V\ bias = 30$ to $0\ v$
[13, 15]	Varactor (SMV2020)	up to 10 GHz	$Rs = 4.1\ \Omega$, $Ct = 0.35$ to 3.2 pF, $V\ bias = 20$ to $0\ v$
[14]	Varactor (MA46H202)	up to 10 GHz	$Rs = 0.8\ \Omega$, $Ct = 2.7$ to 3.3 pF, $V\ bias = 20$ to $0\ v$
[16]	Varactor (SMV1231)	beyond 2.5 GHz	$Rs = 1.5\ \Omega$, $Ct = 0.466$ to 2.35 pF, $V\ bias = 15$ to $0\ v$
[19]	Varactor (SMV1763)	beyond 2.5 GHz	$Rs = 1.5\ \Omega$, $Ct = 0.3$ to 2.35 pF, $V\ bias = 15$ to $0\ v$

urable filter model to direct performance analysis and testing, operating at a frequency of 3.1 GHz – 10.6 GHz with a controllable notch band at 5.2 GHz. After assessing the PIN diode models reported in the literature (as summarized in Table 1), the PIN SMP1340 diode was preferred for this filter design. This diode features a favourable circuit of low series resistance (Rs = 1 Ω), reasonable junction capacitance ($Cj = 0.3$ pF), and high isolation resistance (Rj = 65 kΩ), which are important for maintaining performance over the UWB range while enabling effective notch-band reconfiguration. In addition, its wide frequency band (10 MHz to 10 GHz) and reliable switching features made it the most appropriate PIN diode for the proposed design requirements.

2. Analysis of The Proposed Filter Design

Several topologies were assessed during the initial design phase (more than 20 designs), mostly those based on parallel and series resonators. However, a Grounded Stepped Impedance Resonators (GSIR)-based structure confirmed better performance in simulations in terms of bandwidth and manageable notch implementation. Additionally, this construction presented better support for reconfigurability using PIN diodes without increasing the layout complexity [20,21]. This selection of the proposed structure is shown in Figure 1.

The suggested reconfigurable filter is based on four GSIRs. They serve as the main building blocks to improve the band performance of the proposed UWB filter design. The offered filter was developed using the resonator analysis method. The calculated structure

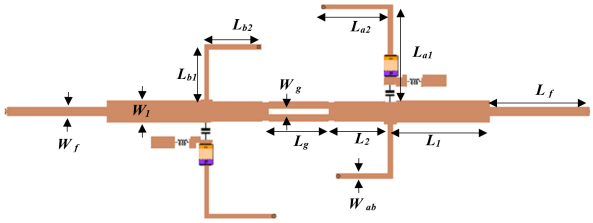

Fig. 1: The Basic Geometry of the Reconfigurable UWB-GSIR Filter.

relates to design in Figure 1 operating at a frequency "f" which describes the desired passband frequency.

The input impedance equation for the analysis method is given by:

$$Z_{in} = Z_0 \frac{Z_l + JZ_0 \tan \beta l}{Z_0 + JZ_l \tan \beta l} \tag{1}$$

The equivalent circuit will be shorted as illustrated in Figure 1, simplifying equation (1) can be written as:

$$Z_{in} = jZ_0 \tan \beta l \tag{2}$$

According to equation (2), the operating frequency that represents the desired passband is:

$$\beta l = \frac{\pi}{2} = \frac{2\pi\sqrt{\varepsilon_{eff}}}{\frac{c}{f}} \times l \tag{3}$$

$$f = \frac{c}{4l\sqrt{\varepsilon_{eff}}} \tag{4}$$

where: l is the length of the transmission line. Z_0 is the characteristic impedance of the transmission line. Z_l is load impedance. c is the speed of light. ε_{eff} is the effective permittivity.

The filter layout contains a central microstrip feedline linked by two pairs of GSIRs to maintain a wide passband and effective impedance matching. Each resonator is connected to the ground by via holes at precisely designed lengths to produce resonance at required frequencies. The input/output ports are coupled by a main feedline with width W_f and length L_f. Each resonator includes low impedance sections expressed by widths W_1 and W_{ab}, lengths L_1, L_2, and stub segments L_{a1}, L_{a2}, L_{b1}, and L_{b2}. These resonators are short-circuited to confirm suitable resonance conditions. The coupling gap between the feedline and the resonators, expressed by W_g and L_g, is used to enhance the quality factor and bandwidth of the filter. Figure 2 shows the current distribution of the proposed reconfigurable UWB filter in addition to the fabricated prototype. The UWB structure with reconfigurability function produces an additional complexity, and the schematic diagram supports an understanding of how the design achieves its proposed performance.

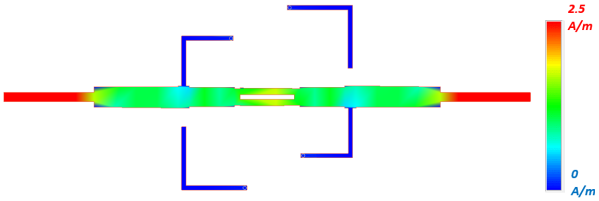

(a)

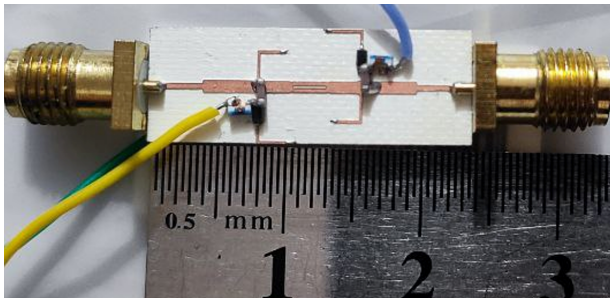

(b)

Fig. 2: The Proposed Reconfigurable UWB Filter, (a) Current Distribution, (b) The Layout Image of the Fabricated Model.

The design of the proposed Reconfigurable Ultra-Wideband (UWB) Filter, as shown in Figure 2, was done by using Advanced Design System (ADS) software [22]. Both schematic simulation and co-simulation tools were applied to confirm the accuracy and performance of the required frequency range. The design procedure can be summarized as follows:

- **The Filter Structure and Parameter Estimation:** including microstrip transmission line and Stepped-Impedance Resonators (GSIRs) sections. Fundamental design equations were used to control transmission line lengths and widths according to the effective permittivity, and target center frequencies.
- **Tuning the Filter Performance:** The Tuning Tool in ADS was dynamically employed to adjust key parameters like (resonator lengths, width, and coupling gaps) to reach effective S-parameter results, specifically at low insertion loss, high return loss, and preferable notch band.
- **Co-Simulation Validation:** When the schematic design achieved acceptable results, co-simulation was employed to integrate electromagnetic effects and the physical geometry of the filter.
- **PIN Diode Positioning:** An important step in achieving the reconfigurability process was selecting the suitable locations for placing the PIN diodes. Various structures were verified, and positioning was enhanced based on how the diode changing the current distribution.

Figure 2 helps as a graphical representation of the filter's design and correspondingly compromises a complete visualization of the current distribution of the proposed filter, enhancing understanding of its dynamic properties.

To clarify the overall structure of the filter design, Figure 3 (a) illustrates the schematic diagram of the proposed UWB - GSIR filter without adding the reconfigurability elements (PIN switches). The resulting filter design responses are demonstrated in Figure 3 (b).

Figure 3 (b) Illustrates the S_{11} curve indicating how much of the input signal is reflected due to impedance mismatch. Across the primary passband from 2.7 GHz to 15 GHz, S_{11} remains consistently below –10 dB, confirming excellent impedance matching and minimal reflection across a wide range. S_{21} presents good performance within the operating frequency indicating the presence of resonant modes introduced by the GSIRs.

The proposed filter design employed the stepped-impedance resonator as a filter's primary structure, to enhance the reconfigurable filter rejection band performance. This model features reconfigurability function by the application of SMP-1430-079 PIN and SMV1405 varactor switches.

The tuning components in Figure 3 are regulated via designated DC biasing circuits. Integrating the DC biasing circuit is a fundamental factor, including categorised components of a PIN diode with a capacitor 50 pF, working as a DC blocking circuit to prevent the DC signal from passing through the input/output RF ports. While an inductor 50 nH operates as an RF

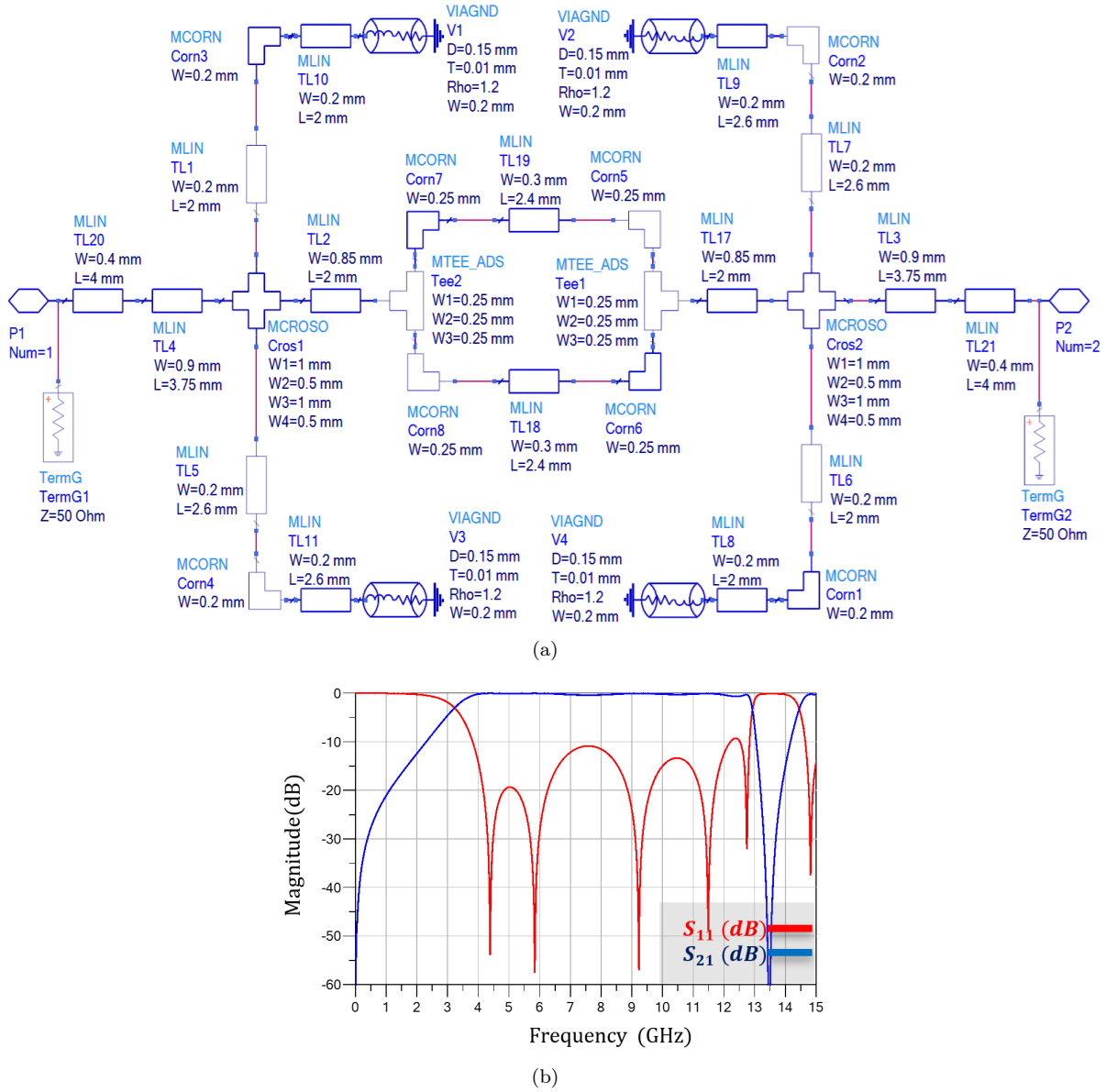

Fig. 3: The Proposed UWB - GSIR Filter, (a) Schematic Diagram, (b) The UWB Filter Response.

choke to confirm separation of the RF signal from the DC supplying circuit. The presence of these controlled elements enables precise regulation over the reconfigurable features of the proposed UWB filters.

The operation of the proposed reconfigurable UWB filter comprises two separated scenarios, with frequencies: 1st operating frequency band at 3.7 GHz – 13 GHz and 2nd operating frequency band at 2.7 GHz – 15 GHz with 5.1 GHz – 5.3 GHz notch band according to the PIN switching state. This designed filter construction is accurately structured on a grounded substrate with a thickness of 0.305 mm. The selected substrate is Rogers (USA Ceramic RO4360) material considered by a relative permittivity of ε_r= 6.15. The precise dimensions that rule the detailed geometry of the filter design are comprehensively detailed in Table 2, providing an observant understanding of the detailed structures.

These dimensions are considerately offered within the schematic diagram, smartly demonstrated in Figures 1 and 3.

To investigate and explain the proposed filtering response, two different procedures were done to clarify the suitable values for the filter design effective parameters.

The GSIR filter design has the same physical dimensions as specified above. With the support of the ADS simulator, two numerical justifications for the pass band performance were conducted to examine and enhance the filtering attitude.

Tab. 2: Geometrical Dimensions Summary for Reconfigurable UWB Filter.

Parameters	h	W_f	W_l	W_g	W_{ab}	L_1	L_2
Dimension (mm)	0.305	0.36	0.9	0.3	0.2	3.75	2
Parameters	L_f	L_g	L_{a1}	L_{a2}	L_{b1}	L_{b2}	
Dimension (mm)	4	2.4	2.6	2.6	2	2	

Figure 4 (a) shows the first numerical scenario when the L_{a1}, L_{a2} varies from 1.8 to 3.4 mm while the remaining parameters are still constant. This study demonstrates that the precise L_{a1}, L_{a2} are 2 mm, which made the operating frequency response performance of 3.7 GHz – 13 GHz, it's clear that reducing the length of L_{a1}, L_{a2} will decrease the UWB frequency band. For the second numerical state of the resonator calculation, where the GSIR parameters L_{b1}, L_{b2} ranges extended from 1.2 to 2.8 mm, as described in Figure 4 (b) while the other filter parameters are continuously unchanging.

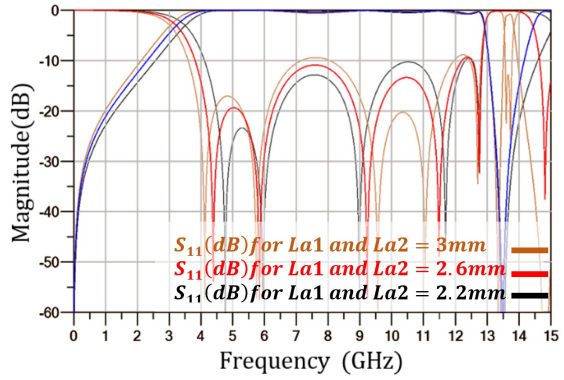

(a)

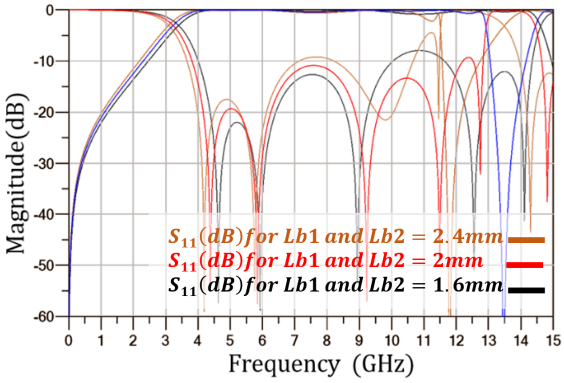

(b)

Fig. 4: Parameter Optimization for GSIR-UWB Filter Design (a) Frequency Response with Variation in L_{a1} and L_{a2} (b) Frequency Response with Variation in L_{b1} and L_{b2}.

This investigation demonstrates that reducing L_{b1} and L_{b2} by 1.8 mm will shift the operating frequency band to the direction of the higher frequencies, increasing the value of L_{b1}, L_{b2} tuning the UWB to the direction of the lower frequencies but at the same time reducing the filter performance at higher frequencies specifically above 6 GHz.

Based on the analysis approach, the multi-actions GSIR is considered to produce an UWB with an extremely desired rejection response. The reconfigurable filter arrangement utilizes four GSIRs coupled directly to input/output feed ports, the feedline width W_f corresponds to the 50 Ω. The proposed L-shaped GSIR is achieved to produce the required filtering response.

3. Simulation and Experimental Results

The reconfigurable UWB filter was fabricated and investigated to confirm the results in the practical scenario. The fabricated filter for practical verification was tested by employing the Agilent / Keysight E5071C Vector Network Analyzer (VNA).

The function of the reconfigurability for the offered reconfigurable UWB filter comprises two PIN switches in the presented filter design. Integrating the DC biasing circuit is a fundamental factor, integrating assorted components of a PIN diode with a capacitor 50 pF performing as DC blocks, while an inductor 50 nH operates as an RF choke. Additionally, the suggested UWB filter can be operated as a notch-tuning filter design employing varactor switches controlled by reverse bias voltage, instead of PIN diodes that are regulated by a forward bias current. It indicates the importance of considering the differences between the DC biasing circuits for the Varactor and PIN diodes separately.

At the same time, Figures 5 and 6 visually describe the function of the reconfigurable elements, and present a graphical illustration of their strategic positioning within the overall filter structure. Besides, Figure 5 offers a detailed understanding of the DC biasing circuit containing the PIN diodes. DC biasing circuits contain capacitors 50 pF as DC blocks and inductors 50 nH as an RF choke, integrated into the schematic diagram of the suggested reconfigurable UWB filter. This detailed illustration clarifies the elements' interaction and spatial configuration within the filter.

Table 3 indicates the switching states of the offered reconfigurable UWB filter utilizing two PIN diodes, in the case of the PIN diode in the ON-state, a series resistance is indicated, equal to 1 Ω. On the other

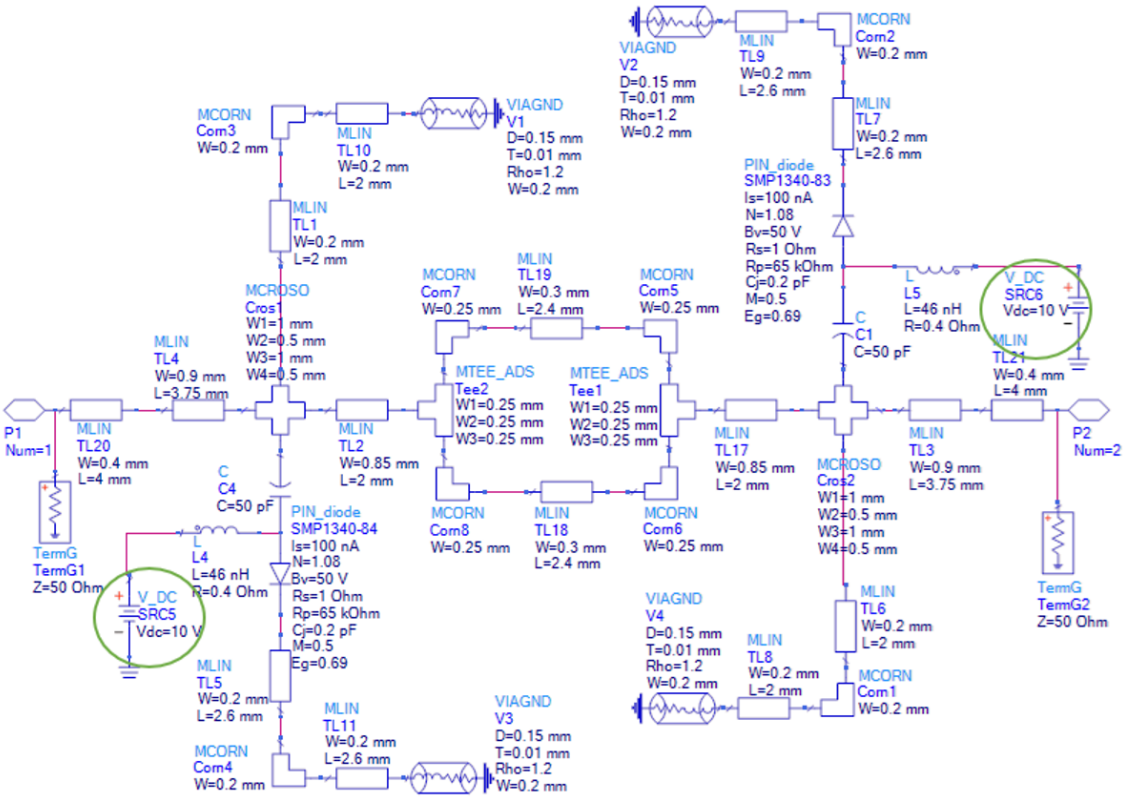

(a)

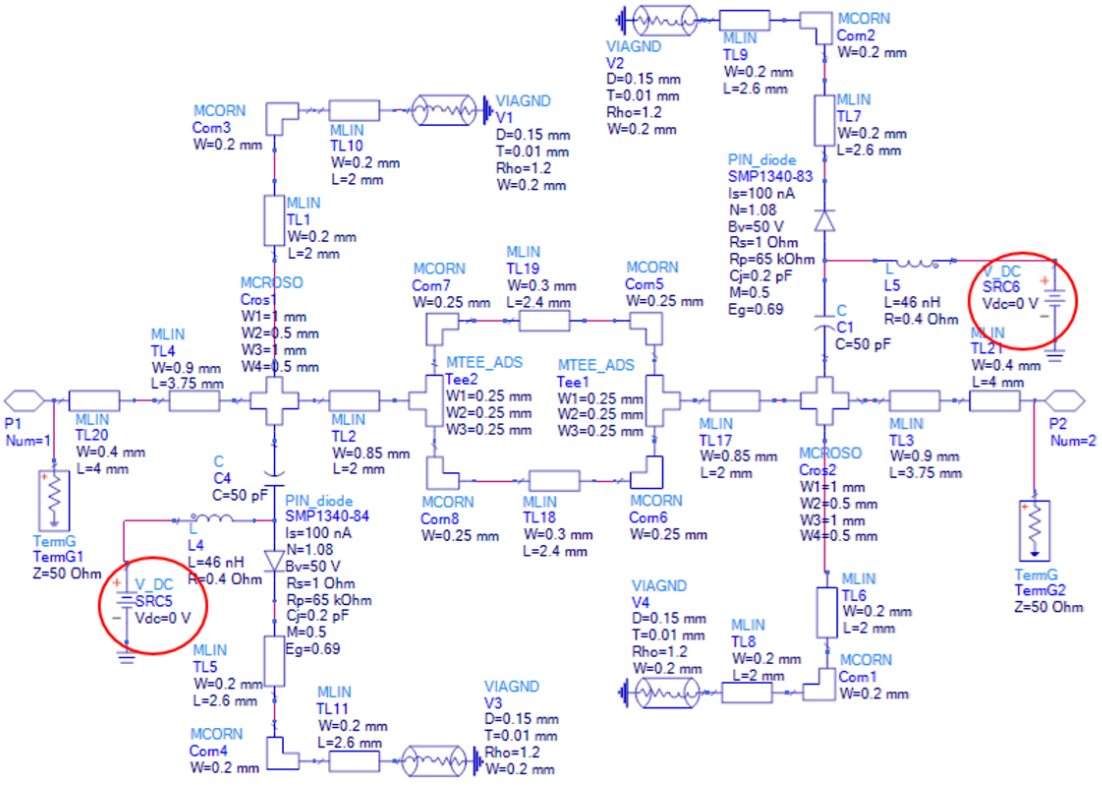

(b)

Fig. 5: Spatial Configuration and DC Biasing Circuit of the Offered Reconfigurable UWB Filter (a) ON-ON state, (b) OFF-OFF state.

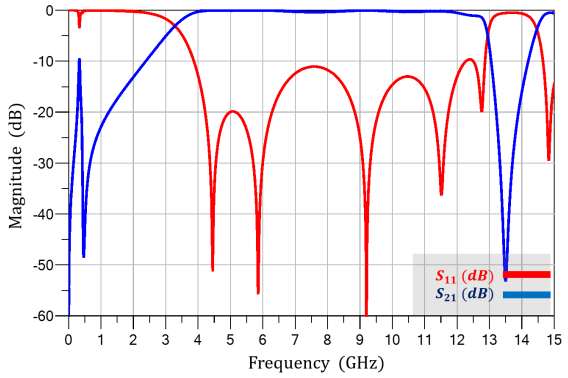

(a)

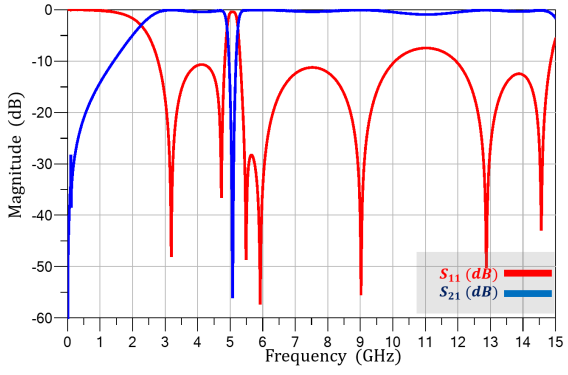

(b)

Fig. 6: Reconfigurable UWB Filter Frequency Response with PIN Switching States, (a) ON-ON state, (b) OFF-OFF state.

hand, for the PIN switch in the OFF state, the switch is characterized by a junction resistance and capacitance established at 100 kΩ and 0.3 pF, respectively.

As shown in Figure 5 (a) and (b), the proposed reconfigurable UWB filter is altered between the 1st operating frequency band at 3.7 GHz – 13 GHz, and 2nd operating frequency band at 2.7 GHz – 15 GHz with 5.1 GHz – 5.3 GHz notch band according to the PIN switching states.

Figure 6 describes the simulation responses S_{21} and S_{11} for the reconfigurable UWB filter in these PIN states, contributing to a complete understanding of the filter's performance in the presence of the switching effects.

According to the results of the insertion loss behavior, it becomes obvious that the filter's skirt selectivity improved by using four separate transmission poles.

The first transmission pole appears within the lower frequency range, precisely located at 4.4 GHz (T_{p1}), showing a magnitude exceeding 51 dB. At the same time, a second transmission pole is located in the middle-frequency range, remarkably at 5.9 GHz (T_{p2}), presenting a magnitude of 58 dB, thus enhancing the

Tab. 3: Switching State of the Offered Microstrip Reconfigurable Band-pass Filter Utilizing PIN.

No.	Switch States	Pass bands (GHz)	B.W (%)	S_{21} (dB)	S_{11} (dB)
1	ON-ON	3.7 $GHz-$ 13 GHz	135	0.9	13 to 58
2	OFF-OFF	2.7 $GHz-$ 15 GHz with 5.1 $GHz-$ 5.3 GHz notch band	179	1.1	8 to 57

selectivity of the filter's response. Furthermore, a third transmission pole becomes observable within the higher frequency range, arising at 9.1 GHz (T_{p3}) and exhibiting a magnitude of 58 dB. While the last transmission pole is located at 11.5 GHz (T_{p4}) with a magnitude of 36 dB.

This arrangement of multiple poles significantly provides an improved level of skirt selectivity, especially by adding a preferable notch band as shown in Figure 6.

Examining the simulated results of S_{21} and S_{11} for the proposed reconfigurable filter in switching state No. 1 when the PIN switch is ON, shows the successful performance of the band-pass frequency with a bandwidth of 9.3 GHz.

The parameters simulation results are:

- S-parameters: start = 0 GHz, Stop 15 = GHz, step = 0.01 GHz.
- MSUB: Roger 4360, Dielectric thickness (H) = 0.305 mm, Relative permittivity (Er) = 6.15, Relative permeability (Mur) = 1.
- Simulate: Tuning Parameters, enable (SRC5, SRC6) for V_{DC} as shown in Figure 5.
- Simulate: Tuning Parameters, enable (other parameters) for numerical validations.
- Plot Traces: dB (S_{11}) dB (S_{21}), trace options = (Linear).

The filter displays good insertion and return losses, evaluating at approximately 0.9 dB/58 dB respectively. Transitioning to the second switching state, when the PIN diodes in the OFF state, the filter is operated as a band-pass filter with a bandwidth of 12.3 GHz including the 5.1 – 5.3 GHz notch band. The simulation results of S_{21} and S_{11} show insertion and return

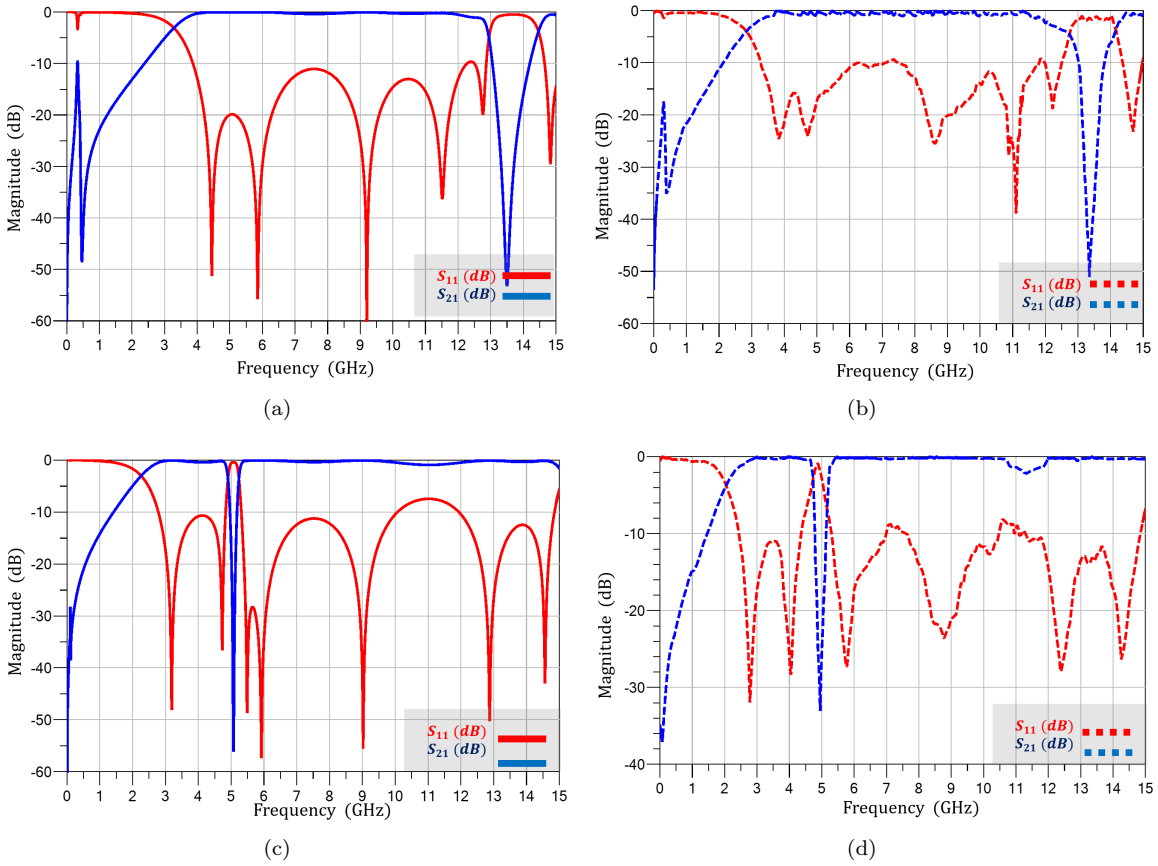

Fig. 7: Validation Results of S_{11} and S_{21} Parameters for, (a) ON-ON state Simulation results, (b) ON-ON state Practical Result, (c) OFF-OFF state Simulation results, (d) OFF-OFF state practical results.

losses of 1.3 dB/57 dB, respectively. However, the presence of a notch band near 500 MHz after adding the PIN diodes highlights the complex interaction between the reconfiguring components and filter performance. The filter structure (without the PIN diodes) shows no such notch band appeared, confirming that the notch at lower frequency is not due to the resonator geometry, but more exactly created blocking capacitor of C=50 pF and an RF choke inductor of L=50 nH were combined to create independent DC control of the PIN diodes. These components affect the lower frequencies as it can be operated as a parasitic resonant circuit (LC circuit can cause resonance, resulting notch band around 500 MHz). The unplanned notch band located outside the operating bandwidth (3.7 GHz – 13 GHz), it does not impact the targeted response.

In addition, the notch band around 500 MHz appears in the ON-ON state after integrating the PIN diodes as shown in Figure 6(a), but is removed in Figure 6(b), which represents the OFF–OFF state. In this condition, both PIN diodes are not conducting, effectively disconnecting the reconfigurable segments from the main filter structure. As a result, the bias lines and related parasitic elements are not connected to the filter, preventing any notches near 500 MHz.

To validate the practical results of the offered reconfigurable filter employing PIN switches, the S_{11} and S_{21} parameters of the manufactured reconfigurable dual passband filter are illustrated in Figure 7.

The Vector Network Analyzer (VNA) Configuration is:

- Frequency bandwidth: Start = 300 KHz, Stop = 15 GHz.
- Intermediate Frequency Bandwidth (IFBW): 70 kHz.
- Number of Points: 201.
- Power: 0 dBm.
- Sweep Type: Lin Freq.
- Sweep Time: 11.184 ms.
- Num of Traces: 2.
- Traces Format: Log Mag.

An obvious match between practical and simulation results is noticeable, verifying the reliability and similarity of the experimental and theoretical results. However, the observed insertion loss in the filter may be

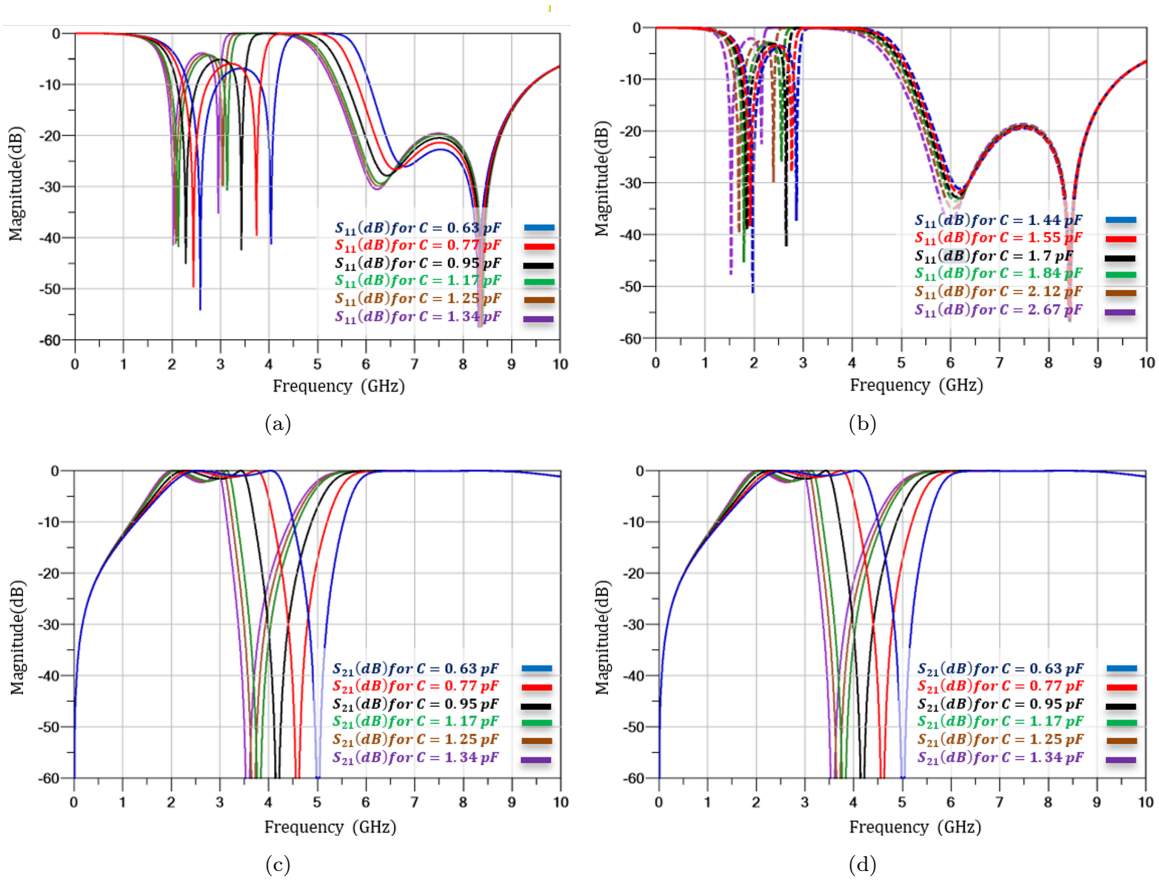

Fig. 8: The Simulation Result of the Tunable UWB Filter Frequency Response with SMV1405 Varactor Switches, (a) S_{11} with (0.63 – 1.34) pF, (b) S_{11} with (1.44 – 2.67) pF, (c) S_{21} with (0.63 – 1.34) pF, (d) S_{21} with (1.44 – 2.67) pF.

attributed to the limitations of the conventional manufacturing procedure, which might have presented additional difficulties and defectiveness in the fabrication procedure, leading to a divergence from the ideal simulated operation.

Also, the frequency shift between the simulated and measured results can be created due to several factors that were not completely taken in the simulation part.

Inaccuracies in printing during the manufacturing process can alter electrical lengths and thus shift resonant frequencies.

The PIN diode and SMA connector soldering may introduce parasitic that shift the frequency response.

Ideal component models in simulation section (including PIN diode and absence of layout parasitics) may not fully represent real-world situations.

These factors contribute to the frequency shift between measurement and simulation.

Figure 8 indicates the simulation result of the UWB frequency band incorporating a tuning notch band that is controlled by the capacitance values for the tuning components. Hence, additional investigation and modification of the manufacturing procedures could moderate this difference and enhance the general performance of the filter.

Table 4 shows the capacitance values of the Varactor diodes according to the reverse bias voltage.

Tab. 4: Typical Capacitance Values for the SMV-1405 Varactor switches.

V (V)	C (pF)	V (V)	C (pF)
0	2.67	3	1.34
0.5	2.12	4	1.25
1	1.84	5	1.17
1.5	1.7	10	0.95
2	1.55	20	0.77
2.5	1.44	30	0.63

The accurate dimensions of the reconfigurable filter circuit, principally when measured at 0.11 λ_g × 0.34 λ_g times the wavelength (λ_g) calculated for a frequency of 7.5 GHz have the greatest significance. This particular consideration of detail focuses on the critical precision desired in the design process to improve the filter's effectiveness within the required frequency spectrum. Problems such as raised insertion loss and

Tab. 5: Comparison with Recently Reported Topologies.

Ref.	Band-pass (GHz)	B.W (%)	S_{11} -(dB)	S_{21} -(dB)	Roll-off rate dB/GHz	Circuit size ($\lambda_g \times \lambda_g$)	Comp-actness (%)	No. of Diodes
[7]	3.1-14	127	15, 25, 20	1, 0.6, 0.3	73	0.43×0.46	81.1	3
[8]	8.5 - 14, 9 - 15.5	47.82, 54.16	20, 30	1.6, 1.2	81.5	0.9×0.96	95.6	4
[10]	0 - 1, 3.4 - 3.8	100, 11	30	1.4	100	0.4×0.32	70.78	1
[12]	5, 10	70	50, 30	2.6, 2.1	13	0.32×0.35	66.6	2
[13]	1.3 - 3.2, 6.5 - 7.5	84, 8	42, 35	0.9, 0.6	32.5	0.45×0.45	81.5	2
[14]	3.35, 5.2	114, 30, 15	20	2.3	12.5	0.56×0.42	84.1	3
[15]	3.4, 3.77	14	22	1.5	45	0.51×0.51	85.6	2
[16]	2 - 6.1, 2.4, 3.5, 5.2	104, 10, 11, 3 11, 3	17, 35, 42, 27, 28	1.7, 1.5, 1.1, 1.4, 0.9	93 93 93	0.53×0.55 0.53×0.55 0.53×0.55	87.1 87.1 87.1	10 10 10
[17]	2.06-2.4, 5.44-5.84	15.3, 7.1	33, 29	1.1, 1.4	15	0.57×0.37	82.3	2
[18]	3.5-10.1	108	15-42	1.2	77	0.64×0.54	89.1	6
[19]	2.25-2.6	2, 4	26, 30	1.2, 1.1	193	0.77×0.61	0.92	9
This work	**3.7 - 13, 2.7 - 15 (with 5.1 - 5.3 notch)**	**135, 179**	**13-58, 8-57**	**0.9, 1.1**	**165**	**0.11×0.34**	**-**	**2**

variations in frequency are essential difficulties related to conventional manufacturing approaches and potential impurities in the substrate material is essential for achieving good performance.

The presented filter was compared with previous related research illustrated in Table 5. Related to other proposed filters, the offered reconfigurable filter supports response for UWB with a miniaturized dimension. The suggested filter offers bandwidth in (9.3 GHz and 12.3 GHz) with only two PIN diodes.

The proposed filter design demonstrates good performance in terms of bandwidth, compactness, and simplicity compared to related works. Accomplishing UWB bandwidths of 135% and 179% with dual-band, along with a notch band operating at 5.1 GHz to 5.3 GHz. In term of filter size, the design achieves better compactness, with a circuit size of 0.11 λ_g × 0.34 λ_g, corresponding to a significant 95.6% reduction in size as compared to [8] and 87.1% reduction compared to [16]. Its design simplicity is demonstrated by the using of only two reconfiguring elements as compared with the related works, while maintaining excellent S_{11} (13–58 dB) and S_{21} (0.9–1.1 dB). Additionaly, the proposed filter achieves a high roll-off rate of 165 dB/GHz, which is considerably sharper than other designs, for instance, it exceeds the roll-off rates reported in [7] (73 dB/GHz), [8] (81.5 dB/GHz), and [16] (93 dB/GHz). This higher roll-off enables improved selectivity and better control for unwanted frequencies. These characteristics make the proposed reconfigurable filter more suitable for modern wireless applications, including UWB communication, where compactness, performance, and tunability function are essential.

4. Conclusion

This research provides a detailed comparative analysis of reconfigurable microstrip filters, focusing on the effect of SMP-1340-079 PIN and SMV1405 Varactor switches, in combination with capacitors and inductors for the DC biasing circuit, on general filter performance. The study discovers the influence of these reconfigurable components on insertion loss and return loss, providing a complete understanding of their functions in filter design. The study integrates the theoretical modeling and practical testing to justify proposed constructs with the aid of a Reconfigurable UWB Filter design. The reconfigurable band-pass filter design contains four GSIRs, strategically confirmed to operate at two separate frequencies: "f_1" at 3.7-13 GHz and "f_2" at 2.7-15 GHz, with 5.1-5.3 GHz notch band. This research not only develops theoretical insights into recon-

figurable microstrip filters but also designs a practical model that can operate on a UWB operating frequency with a compact size while applying the reconfigurability function. However, the suggested reconfigurable filter deals with challenges in practical operation due to fabrication limitations. The conventional manufacturing procedure influences higher insertion losses and frequency shifts, affecting the overall performance of the reconfigurable filters.

Author Contributions

S. M. developed the theoretical formalism, performed the analytic calculations and performed the numerical simulations. Both M. N. and R. T. authors contributed to the final version of the manuscript. M. N. and R. T. supervised the work.

References

[1] HAMMED, R. T., D. MIRSHEKAR-SYAHKAL. Miniaturized high-order UWB bandpass filter using third-order E-shape microstrip structure. *2012 IEEE/MTT-S International Microwave Symposium Digest, Montreal, QC, Canada*. 2012, pp. 1-3. DOI: 10.1109/MWSYM.2012.6258259.

[2] SATISH, C. G., M. KUMAR, R. S. MEENA. Design & analysis of a microstrip line multi band UWB filter. *AEU - International Journal of Electronics and Communications*. 2016, vol. 70, iss. 11, pp. 1556-1564. DOI: 10.1016/j.aeue.2016.09.014.

[3] FARIS, H. A., G. H. ALYAMI, H. N. SHAMAN. Parallel-Coupled-Line Bandpass Filter with Notch for Ultra-Wideband (UWB) Applications. *Applied Sciences*. 2013, vol. 11, no. 11. DOI: 10.3390/app13116834.

[4] SENATHIPATHI, U., K. SHAMBAVI. Compact Single Notch UWB Bandpass Filter with Metamaterial and SIW Technique. *Progress In Electromagnetics Research Letters*. 2024, vol. 117, pp. 41-46. DOI: 10.2528/PIERL23113004.

[5] QIN, M., et al. Varactor-Based Continuously Tunable Microstrip Bandpass Filters: A Review, Issues and Future Trends. *IEEE Access*. 2024, vol. 12, pp. 57443-57457. DOI: 10.1109/ACCESS.2024.3383788.

[6] ISLAM, H., S. DAS, T. BOSE, T. ALI. Diode Based Reconfigurable Microwave Filters for Cognitive Radio Applications: A Review. *IEEE Access*. 2020, vol. 8, pp. 185429-185444. DOI: 10.1109/ACCESS.2020.3030020.

[7] LI, Y., W. LI, Q. YE. A Reconfigurable Triple-Notch-Band Antenna Integrated with Defected Microstrip Structure Band-Stop Filter for Ultra-Wideband Cognitive Radio Applications. *International Journal of Antennas and Propagation*. 2013, pp. 1–13. DOI: 10.1155/2013/472645.

[8] ALQAISY, M., et al. Switchable square ring bandpass to bandstop filter for ultra-wideband applications. *International Journal of Microwave and Wireless Technologies*. 2017, vol. 9, no. 1, pp. 51-60. DOI: 10.1017/S1759078715001373.

[9] ABDALLA, M. A., D. K. CHOUDHARY, R. K. CHAUDHARY. A compact reconfigurable bandpass/lowpass filter with independent transmission zeros based on generalized NRI metamaterial. *International Journal of RF and Microwave Computer-Aided Engineering*. 2020, vol. 30. DOI: 10.1002/mmce.22074.

[10] AL-YASIR, Y., et al. Novel and Very Compact Reconfigurable Bandpass to Lowpass/Bandpass Microstrip Filter with Wide-stopband Restriction for 5G Communications. *Proceedings of the 1st International Multi-Disciplinary Conference Theme: Sustainable Development and Smart Planning, IMDC-SDSP 2020, Cyperspace*. 2020, pp. 28-30. DOI: 10.4108/eai.28-6-2020.2298131.

[11] KINGSLY, S., et al. Switchable Resonator Based Reconfigurable Bandpass / Bandstop Microstrip Filter. *International Journal of Electronics*. 2021, vol. 108, no. 9, pp. 1610–1622. DOI: 10.1080/00207217.2021.1908613.

[12] ALLANIC, R., et al. On-Chip Bandstop to Bandpass Reconfigurable Filters Using Semiconductor Distributed Doped Areas (ScDDAs). *Electronics*. 2022, vol. 11, no. 20. DOI: 10.3390/electronics11203420.

[13] MEHUL, T., R. P. PRAVIN, S. HITESH. Reconfigurable Dual Wideband Bandstop-Bandpass Switching Filter Using PIN Diodes. *International Journal of Microwave & Optical Technology*. 2023, vol. 18, iss. 4.

[14] CUI, J., A. ZHANG, Z. WU, S. YAN. A frequency reconfigurable filtering antenna based on stepped impedance resonator. *Journal of Electromagnetic Waves and Applications*. 2020, vol. 34, no. 5, pp. 571–5800. DOI: 10.1080/09205071.2020.1719212.

[15] SYED, H. S., et al. Design of Reconfigurable Wide Band Pass Filter. *International Journal of Future Generation Communication and Networking*. 2020, vol. 13, pp. 1376–1382.

[16] BANDYOPADHYAY, A., P. SARKAR, T. MONDAL, R. GHATAK. A Dual Function Reconfigurable Bandpass Filter for Wideband and Tri-Band Operations. *IEEE Transactions on Circuits and Systems II: Express Briefs*. 2021, vol. 68, no. 6, pp. 1892-1896. DOI: 10.1109/TCSII.2020.3047873.

[17] ALAZEMI, A. J., D. H. ALMATAR. A Frequency-Reconfigurable Dual-Band RF Crossover Based on Coupled Lines and Open Stubs. *Electronics*. 2024, vol. 13, no. 13. DOI: 10.3390/electronics13132641.

[18] CHOWDHURY, A., P. RANJAN. A Novel Stepped-Flower Shaped UWB Frequency Reconfigurable Printed Filtering Antenna Using PIN Diodes with Trackable Notch-Band for Mid-5G Band & X-Band Applications. *MAPAN*. 2024, vol. 39, pp. 1031–1044. DOI: 10.1007/s12647-024-00778-7.

[19] MOHAMED, G., J. ZBITOU, M. HEFNAWI, F. AYTOUNA. A novel configuration of reconfigurable bandpass filter based on varactor diodes. *e-Prime - Advances in Electrical Engineering, Electronics and Energy*. 2025, vol. 1. DOI: 10.1016/j.prime.2024.100889.

[20] HAMMED, R. T., Z. M. ABDUL-JABBAR. Multilayered stepped impedance loaded-resonator for compact dual-band rejection filter design. *Electromagnetics*. 2017, vol. 37, no. 8, pp. 493–499. DOI: 10.1080/02726343.2017.1392717.

[21] RUAA, A. D., Y. S. MEZAAL, H. J. A. KAREEM, Z. K. HUESSEIN. New microstrip multiband filter for modern wireless applications using Kappa substrate material. *Materials Today: Proceedings*. 2022, vol. 61, pp. 1038-1042. DOI: 10.1016/j.matpr.2021.10.299.

[22] Electromagnetic, Advanced Design System (ADS). *Santa Rosa, CA 95403-1738 United States: Agilent Technologies*. 2017.